that in complex **3**. The weakening of this bond explains the unexpected racemization[39] that resulted during persistent efforts to prepare the Schiff base complex with the biologically more relevant L-tyrosine.[40] In addition to N(2)–C(9), C(3)–C(8) also shows partial double-bond character. The pyridine ring shows two short bonds of 1.354 (9) and 1.338 (11) Å in agreement with a quinoid structure as in the case of a salicylaldehyde–glycine complex.[41] The C(1)–C(6) bond length is almost normal.[42]

Acknowledgment. We thank the reviewers for their valuable comments.

Supplementary Material Available: Tables S-1–S-9, listing complete positional and thermal parameters, including those of the hydrogen atoms, bond distances and angles involving hydrogen atoms, least-squares planes, selected torsion angles and asymmetry parameters, possible H bonds, and intermolecular short contacts (15 pages); a table of observed and calculated structure factors (18 pages). Ordering information is given on any current masthead page.

(39) Details of this work will be published elsewhere.
(40) To our knowledge, the only Schiff base metal complex having an L-amino acid to be crystallographically characterized is Zn^{II}(PL-L-valine).[6a] A comparison of this structure with the corresponding Ni^{II}-(PL-DL-valine) complex showed that the Schiff base moiety has a similar geometry in both complexes.
(41) Bkouche-Waksman, I.; Barke, J. M.; Kvick, A. *Acta Crystallogr., Sect. B: Struct. Crystallogr., Cryst. Chem.* **1988**, *B44*, 595.
(42) This shows that hyperconjugative effects[43] may not be playing an important role here as noted in the Cu(PLP-valine) complex.[37]
(43) Maslen, H. S.; Waters, T. N. *Coord. Chem. Rev.* **1975**, *17*, 137.

Contribution from the Departamento de Química, Faculdade de Filosofia, Ciências e Letras de Ribeirão Preto, Universidade de São Paulo, Av. Bandeirantes 3900, 14.049-Ribeirão Preto, SP, Brazil

Photoaquation of *cis*-Bis(azine)tetraammineruthenium(II) Complexes, *cis*-$Ru(NH_3)_4(L)(L')^{n+}$ [1]

Luiz Alfredo Pavanin,[2a] Zênis Novais da Rocha,[2a] Ernesto Giesbrecht,[2b] and Elia Tfouni*,[2c]

Received July 23, 1990

Near-UV–visible range photolysis of *cis*-$Ru^{II}(NH_3)_4(L)_2$ (L = pyridine (py), 4-picoline (4-pic), isonicotinamide (isn), or 4-acetylpyridine (4-acpy)) and *cis*-$Ru^{II}(NH_3)_4$(isn)(L) (L = py, 4-pic, pyrazine, or 4-acpy) leads to isn, L, and ammonia aquation. The complexes were irradiated at 313, 365, 405, 436, 480, and 519 nm, in acidic (pH 3.5–4.0) aqueous solution and with $\sim 10^{-3}$ M Ru complex concentration. The cis complexes have ligand field (LF) and metal-to-ligand charge-transfer (MLCT) states as the lowest energy excited states. The relative yields of the photoreactions of the cis complexes show patterns consistent with the excited-state "tuning" model proposed to explain photochemical properties of the pentaammine analogues, $Ru^{II}(NH_3)_5(L)$, which undergo photosubstitution when LF is the lowest energy excited state, as is also the case for the trans complexes. For each cis complex, a fixed ratio of released ligands is observed at all irradiation wavelengths studied, this being a strong evidence that the observed photoreactions occur from one single LF excited state, or an ensemble of equilibrated LF excited states of the same electronic configuration. Ligands are more easily labilized along the axis with the weaker π-acceptor ability. For a particular axis, the ligand with lower π-acceptor ability is more easily labilized.

Introduction

The photosubstitution reactions of d^6 transition-metal ion species that have metal-to-ligand charge-transfer (MLCT) and ligand field (LF) states as the lowest energy excited states (LEES) have been rationalized in terms of the excited-state "tuning" model.[3,4] According to this model, the relatively photosubstitution "reactive" complexes have a LF state as the LEES, and those that are relatively "unreactive" have a MLCT state as the LEES. This model was initially proposed to explain the photosubstitution chemistry of pentaammineruthenium(II) complexes $(NH_3)_5Ru(L)^{n+}$ (where L is an aromatic nitrogen ligand) but has been extended to photoreactions of other systems.[5] Although the MLCT states of $Ru(bpy\text{-}X)_y^{2+}$, $Ru(bpy)_x(py\text{-}X)_y^{2+}$, and related bipyridine complexes are generally the LEES, the "tuning" model, which can also consider the effect of substituents on the relative energies of their long-lived but relatively unreactive MLCT states and of the substitution labile LF states, can explain much of the photosubstitution chemistry of these species.[6]

Ammineruthenium(II) complexes of unsaturated aromatic nitrogen heterocycles have LF and MLCT as LEES of comparable energies. The energy of the MLCT states in these complexes is highly dependent on the substituents on the coordinated heterocycle on the solvent, while the LF energy has been assumed to be much less sensitive.[3,7] Variation of either of these parameters will determine the nature of the LEES (LF or MLCT) and, thus, "tune" the photoreactivity.[3,4]

The $Ru^{II}(NH_3)_5(L)^{n+}$ (L = pyridine-like ligands) complexes show only one MLCT absorption band (in the visible region),[3a,8] while the *trans*-$Ru^{II}(NH_3)_4(L)(L')^{n+}$ ions display two MLCT bands, with the lower energy one (MLCT-1) being the more intense.[6,9] The absorbance of the higher energy MLCT band (MLCT-2) of *trans*-$Ru^{II}(NH_3)_4(L)(L')^{n+}$ is enhanced when $L \neq L'$.[6,9] Earlier work from these laboratories has shown that in the case of these trans complexes there appeared to be no special character assignable to the photochemistry resulting when the higher energy band (MLCT-2) is irradiated[7]—that is, the product distributions were the same as seen at longer wavelength excitation. Although the higher energy excitations did in some cases show high quantum yield values, these data are clearly consistent with explanations based on the "tuning" model.

(1) (a) Taken in part from: Pavanin, L. A. D.Sc. Thesis, Instituto de Química da Universidade de São Paulo, 1988. (b) Presented partly at the Third Encontro Brasileiro de Fotoquímica e Fotobiologia, Rio de Janeiro, Brazil, 1986, Second Encontro Latino-Americano de Fotoquímica e Fotobiologia, São Carlos, Brazil, 1988, and VIII International Symposium on the Photochemistry and Photophysics of Coordination Compounds, Santa Barbara, CA, 1989.
(2) (a) Present address: Departamento de Química, Universidade Federal de Uberlândia. (b) Present address: Instituto de Química da Universidade de São Paulo. (c) Departamento de Química da Faculdade de Filosofia, Ciências e Letras de Ribeirão Preto da Universidade de São Paulo.
(3) (a) Malouf, G.; Ford, P. C. *J. Am. Chem. Soc.* **1977**, *99*, 7213. (b) Malouf, G.; Ford, P. C. *Ibid.* **1974**, *96*, 601. (c) Malouf, G. Ph.D. Thesis, University of California, Santa Barbara, 1977.
(4) Ford, P. C. *Rev. Chem. Intermed.* **1979**, *2*, 267.
(5) (a) Wrighton, M. S.; Abrahamson, H. B.; Morse, D. L. *J. Am. Chem. Soc.* **1976**, *98*, 4105. (b) Abrahamson, H. B.; Wrighton, M. S. *Inorg. Chem.* **1979**, *17*, 3385. (c) Figard, J. E.; Petersen, J. D. *Ibid.* **1978**, *17*, 1059.
(6) (a) Caspar, J. V.; Meyer, T. J. *Inorg. Chem.* **1983**, *22*, 2444. (b) Allen, G. H.; White, R. P.; Rillema, D. P.; Meyer, T. J. *J. Am. Chem. Soc.* **1984**, *106*, 2613. (c) Ross, H. B.; Boldaji, M.; Rillema, D. P.; Blanton, C. B.; White, R. P. *Inorg. Chem.* **1989**, *28*, 1013.
(7) Tfouni, E.; Ford, P. C. *Inorg. Chem.* **1980**, *19*, 72.
(8) Ford, P. C.; Rudd, De F. P.; Gaunder, R.; Taube, H. *J. Am. Chem. Soc.* **1968**, *90*, 1187.
(9) Bento, M. L.; Tfouni, E. *Inorg. Chem.* **1988**, *27*, 3410.

0020-1669/91/1330-2185$02.50/0

The *cis*-$Ru^{II}(NH_3)(L)(L')^{n+}$ complexes display two visible range MLCT absorption bands of similar intensities.[10] In some analogous trans complexes, the two MLCT bands do not overlap, but in the cis complexes, this is generally the case, and, as a result, some cis complexes absorb in a wide wavelength range in the near-UV–visible region. Thus, we decided to investigate the quantitative photochemical properties of some *cis*-$Ru^{II}(NH_3)_4(L)(L')^{n+}$ complexes, which allow irradiation at several different wavelengths.

Experimental Section

Chemicals and Reagents. Pyridine (py) (Aldrich), 4-picoline (4-pic) (Aldrich), and 4-acetylpyridine (4-acpy) (Aldrich) were distilled under reduced pressure before use. Isonicotinamide (isn) (Aldrich) was recrystallized from hot water, with activated charcoal, before use. Pyrazine (pz) (99.9%, Gold Label) (Aldrich) was used as supplied. $NaBF_4$ was recrystallized from hot water before use. Ether, methanol, ethanol, and acetone were purified before use. "Ruthenium trichloride" ($RuCl_3 \cdot 3H_2O$) (Strem) was the starting material for ruthenium complexes syntheses. Doubly distilled water was used throughout this work. All other materials were reagent grade and were used without further purification.

Syntheses. *cis*-$[Ru(NH_3)_4(isn)(L)](BF_4)_2$ complexes, where L = py, 4-pic, pz, or 4-acpy, were synthesized as previously described.[10] *cis*-$[Ru(NH_3)_4(py)_2](BF_4)_2$ was synthesized according to the literature procedure.[11] We were unable to synthesize *cis*-$[Ru(NH_3)_4(isn)_2](BF_4)_2$ by this procedure, so the general procedure to synthesize *cis*-$[Ru(NH_3)_4(isn)L](BF_4)_2$ was used with isn as L. *cis*-$[Ru(NH_3)_4(4\text{-pic})_2]Cl_3 \cdot H_2O$ and *cis*-$[Ru(NH_3)_4(4\text{-acpy})_2]Cl_3 \cdot H_2O$ were synthesized by the following procedure: A 100-mg sample of *cis*-$[RuCl_2(NH_3)_4]Cl$ was dissolved in 5 mL of previously deaerated water. Zn(Hg) was added to the solution, with continuous argon bubbling, in the dark. An excess of L (4-pic or 4-acpy) ligand was then added. After 2 h of reaction in the dark, the Zn(Hg) was removed, and 1.5 mL of 3 M HCl was added, followed by some drops of 30% H_2O_2. Acetone was then added, and the mixture was cooled for ca. 12 h. The *cis*-$[Ru(NH_3)_4L_2]Cl_3 \cdot H_2O$ formed was collected by filtration, washed with acetone and ether, and then vacuum dried at room temperature. Yields in these cases were about 45%. These two Ru(III) complexes were reduced "in situ" to generate the corresponding Ru(II) complex to be studied. The bis(pyridine) complex was also synthesized in the form of *cis*-$[Ru(NH_3)_4(py)_2]Cl_3 \cdot H_2O$ in order to check if the procedure of starting from a Ru(III) complex was working. Studies with bis(pyridine) complex were performed with both samples, *cis*-$[Ru(NH_3)_4(py)_2]Cl_3 \cdot H_2O$ to generate the corresponding *cis*-$Ru(NH_3)_4(py)_2^{2+}$ and *cis*-$[Ru(NH_3)_4(py)_2](BF_4)_2$, yielding practically the same results.

Elemental Analysis. Carbon, hydrogen, and nitrogen microanalyses were performed at the Instituto de Química da Universidade de São Paulo. Anal. Calcd for *cis*-$[Ru(NH_3)_4(py)_2]Cl_3 \cdot H_2O$: C, 26.6; N, 18.6; H, 5.4. Found: C, 26.5; N, 18.3; H, 5.5. Calcd for *cis*-$[Ru(NH_3)_4(4\text{-pic})_2]Cl_3 \cdot H_2O$: C, 30.0; N, 17.5; H, 5.9. Found: C, 30.2; N, 17.4; H, 6.0. Calcd for *cis*-$[Ru(NH_3)_4(4\text{-acpy})_2]Cl_3 \cdot H_2O$: C, 31.4; N, 15.6; H, 5.3. Found: C, 31.4; N, 15.4; H, 5.4.

Spectra. Electronic spectra were recorded at room temperature with a Beckman UV-5270, a Varian 634-S, or a Varian DMS-80 recording spectrophotometer using quartz cells. Solutions used to measure extinction coefficients were prepared gravimetrically with quantitative dilution.

Photolysis Procedures. These are quite similar to previously described procedures.[7] Irradiations at 313, 365, 405, 436, 480, and 519 nm were carried out by using an Osram 150 W/1 xenon lamp in an Oriel Model 8500 Universal arc lamp source with an Oriel interference filter for monochromatization (band-pass ~10 nm), an infrared filter, and a thermostated cell holder. Photolyses were carried out in aqueous solutions, at pH 3.5–4.0 (with HCl), of $\sim 10^{-3}$ M Ru complex concentration. Ferrioxalate actinometry was used for light intensity measurements at 313, 366, and 405 nm, and Reinecke ion actinometry was used for measurements at 436, 480, and 519 nm.

Solutions for photolyses and dark reactions were prepared and deaerated with purified argon in a Zwickel flask[12] and transferred to the 2.0-cm path-length quartz cells. A 0.5-mL sample of this solution diluted to 10.0 mL and stored in the dark was used as a spectrophotometric blank. During photolysis, the solution was stirred by a small magnetic bar in the cell. All photolyses were carried out at 25.0 ± 0.1 °C. For spectroscopic quantum yield determinations, the reactions under photolysis were monitored periodically by recording the UV–vis spectra. Analogous reaction mixtures allowed to react in the dark, under the same conditions of the photolyzed solutions, displayed either no observable or just negligible spectral changes. Procyon PHD-10 or Metrohm Model E-500, both digital, pH meters calibrated against buffers were employed to evaluate pH changes as the result of photolysis. The major cause of such changes was the release of ammonia from the Ru(II) coordination sphere. After photolysis, the pH values of the dark and irradiated solutions were determined, and the quantum yields were calculated from pH differences taking into account the pK_a's of the other ligands aquated. The quantities of the organic ligands aquated, py, 4-pic, pz, isn, and 4-acpy released into solution, thermally or photochemically, were determined by ion-exchange chromatography. Typically 3.5 mL of the photolyzed solution is adjusted to pH ~2 with HCl, oxidized with some drops of 30% H_2O_2 and charged onto a Dowex 50 W-X4, 200–400 mesh column. The ligands were eluted with different eluents depending on the identity of L and L'. py, 4-acpy, and isn, from the complexes *cis*-$Ru(NH_3)_4(L)_2^{2+}$ were eluted with 0.6 M NaCl solutions at pH 2 (with HCl). 4-pic, from *cis*-$Ru(NH_3)_4(4\text{-pic})_2^{2+}$ was eluted with 0.9 M NaCl solutions at pH 2 (with HCl). Isonicotinamide and 4-picoline, from *cis*-$Ru(NH_3)_4(isn)(4\text{-pic})^{2+}$, were eluted with 0.05 M NaCl solutions at pH 3.9 (with HCl) and 0.6 M NaCl solutions at pH 2 (with HCl), respectively. Pyrazine and isonicotinamide from *cis*-$Ru(NH_3)_4(isn)(pz)^{2+}$, were eluted with water and 0.6 M NaCl solutions at pH 2 (with HCl), respectively. Concentrations of the ligands in eluent aliquots were determined from absorbance measurements in a 1.00-cm path-length cell. Since resolution was not good enough under the conditions tried in these experiments to achieve a good separation, isn and 4-acpy from *cis*-$Ru(NH_3)_4(isn)(4\text{-acpy})^{2+}$ were eluted together with 0.9 M NaCl solutions at pH 1 (with HCl) and their concentrations were calculated from absorbance measurements at two different wavelengths, knowing the molar extinction coefficients of each of these species at these two wavelengths. For similar reasons, the same method was applied in the determination of isn and py from *cis*-$Ru(NH_3)_4(isn)(py)^{2+}$; these ligands were eluted with 0.9 M NaCl solutions at pH 1 (with HCl). The elution conditions and procedures were checked by using stock solutions of the ligands and of the appropriate mixture in concentrations near those expected for the photoreaction solutions. Recoveries of ligands in these checks averaged ~95%.

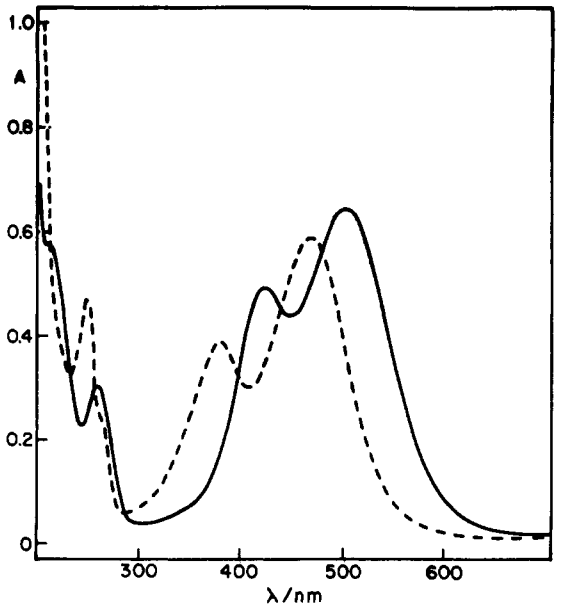

Figure 1. Electronic spectra in dilute aqueous solutions: (—) *cis*-$Ru(NH_3)_4(isn)(4\text{-acpy})^{2+}$, BF_4^- salt; (- -) *cis*-$Ru(NH_3)_4(isn)(py)^{2+}$, BF_4^- salt.

Results

Table I summarizes the electronic spectral properties of the *cis*-$Ru(NH_3)_4(L)(L')$ complexes studied in this work, along with some other related complexes. Figures 1 and 2 show the spectra

(10) Pavanin, L. A.; Giesbrecht, E.; Tfouni, E. *Inorg. Chem.* **1985**, *24*, 4444.
(11) Ford, P. C.; Sutton, C. *Inorg. Chem.* **1969**, *8*, 1544.
(12) It is an all-glass apparatus designed to prepare a solution under a desired atmosphere, to bubble argon (in our experiments) into this solution, and to transfer it to the quartz cells. There is a drawing of such a flask in ref 13.
(13) Gaunder, R. G. Ph.D. Thesis, Stanford University, Stanford, CA, 1969.
(14) Zwickel, A. M.; Creutz, C. *Inorg. Chem.* **1971**, *10*, 2395.
(15) Gaunder, R. G.; Taube, H. *Inorg. Chem.* **1970**, *9*, 2627.

Table I. Electronic Spectra of *cis*-$Ru(NH_3)_4(L)(L')^{n+}$ Complexes and Analogous *trans*-$Ru(NH_3)_4(L)(L')^{n+}$ and $Ru(NH_3)_5(L)^{n+}$ in Aqueous Solution[a]

complex	λ_{max} (log ϵ)[b] MLCT-1	MLCT-2	IL	ref
cis-$Ru(NH_3)_4(isn)(4\text{-pic})^{2+}$	467 (4.05)	371 (3.85)	246 (3.87), 257 (sh)	10
cis-$Ru(NH_3)_4(isn)(py)^{2+}$	466 (4.01)	378 (3.83)	247 (3.90), 257 (sh)	10
cis-$Ru(NH_3)_4(4\text{-acpy})(isn)^{2+}$	503 (4.13)	426 (4.02)	262 (3.81), 218 (sh)	10
cis-$Ru(NH_3)_4(isn)(pz)^{2+}$	476 (4.14)	405 (3.98)	257 (4.05)	10
cis-$Ru(NH_3)_4(4\text{-acpy})_2^{2+}$[c]	518 (4.03)	442 (3.90)	264 (3.79)	this work
cis-$Ru(NH_3)_4(4\text{-pic})_2^{2+}$[c]	398 (3.93)	350 (3.87)	243 (3.92)	this work
cis-$Ru(NH_3)_4(py)_2^{2+}$	407 (3.91)	366.5 (3.85)	245 (3.90)	this work
	410 (3.90)	375 (3.81)	245 (3.86)	11
cis-$Ru(NH_3)_4(isn)_2^{2+}$	478 (4.13)	413 (4.01)	257 (3.88)	10
	478 (4.14)	413 (4.02)	257 (3.89)	13
cis-$Ru(NH_3)_4(pz)_2^{2+}$	471	400	255	this work
	469	398		14
trans-$Ru(NH_3)_4(4\text{-acpy})_2^{2+}$	532 (4.32)	383 (3.27)	270 (3.80), 221 (4.18)	9
trans-$Ru(NH_3)_4(pz)_2^{2+}$	487 (4.32)	375 (3.02)	256 (4.08)	7
trans-$Ru(NH_3)_4(pzH)_2^{4+}$	626 (4.46)	~440 (2.93)	282 (3.95), 258 (sh) (3.81)	7
trans-$Ru(NH_3)_4(isn)(py)^{2+}$	470 (4.18)	363 (3.42)	260 (3.54), 246 (3.85)	9
$Ru(NH_3)_5(4\text{-pic})^{2+}$	397 (3.89)		244 (3.67)	11
$Ru(NH_3)_5(pz)^{2+}$	472 (4.03)		253 (3.78)	3
$Ru(NH_3)_5(pzH)^{3+}$	529 (4.08)		272 (3.81)	3
$Ru(NH_3)_5(4\text{-acpy})^{2+}$	523 (3.97)		271 (3.53), 223 (3.76)	3
$Ru(NH_3)_5(isn)^{2+}$	479 (4.06)		260 (3.66)	15
$Ru(NH_3)_5(py)^{2+}$	407 (3.89)		244 (3.67)	10
	407 (3.89)		244 (3.66)	8

[a] BF_4^- salts in each case, except where noted. [b] λ_{max} in nm; ϵ is the molar extinction coefficient in M^{-1} cm^{-1}. [c] Generated in solution by reduction of the corresponding *cis*-$[Ru(NH_3)_4(L)_2]Cl_3 \cdot H_2O$ complex.

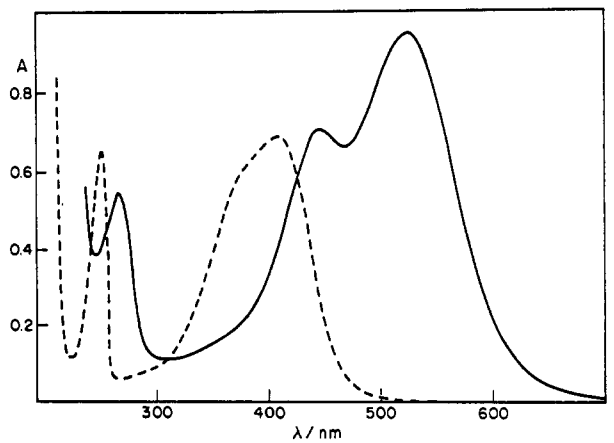

Figure 2. Electronic spectra in dilute aqueous solutions: (—) *cis*-$Ru(NH_3)_4(4\text{-acpy})_2^{2+}$, Cl^- salt; (- -) *cis*-$Ru(NH_3)_4(py)_2^{2+}$, BF_4^- salt.

of some cis complexes. These complexes display UV and visible region absorption bands assigned as intraligand (IL) bands, bands of ligand $\pi-\pi^*$ parentage, and MLCT bands, respectively.

Near-UV–visible range photolysis in acidic aqueous solutions of each *cis*-$Ru^{II}(NH_3)_4(L)_2$ (L = py, 4-pic, isn, or 4-acpy) or *cis*-$Ru^{II}(NH_3)_4(isn)(L)$ (L = py, 4-pic, 4-acpy, or pz) complex leads to competitive photoaquation of L', L, and ammonia (eq 1).

$$cis\text{-}Ru^{II}(NH_3)_4(L)(L') + H_2O \xrightarrow[H^+]{h\nu} \begin{cases} Ru^{II}(NH_3)_4L(OH_2) + L' \\ Ru^{II}(NH_3)_4(OH_2)(L') + L \\ Ru(NH_3)_3(OH_2)(L)(L') + NH_3 \end{cases} \quad (1)$$

Tables II and III summarize the quantum yields of the ligand photoaquation observed when the aqueous *cis*-$Ru^{II}(NH_3)_4(L)(L')$ ions are irradiated in the visible–near-UV ranges. No photooxidation to Ru(III) was seen in this photolysis wavelength range in deaerated solutions. As was found earlier for the pentaammine[3] and *trans*-tetraammine[7] analogues, following the photolysis-induced decreases in the MLCT absorption gives a qualitative estimate of the relative reactivity of a particular complex under the specific conditions. However, since the spectral quantum yields, in these cases, are uninformative regarding the relative importance of the different photoaquation pathways, the quantum yields were obtained from the combination of ion-exchange chromatography and pH measurements. Stereochemistries of Ru(II) products were not determined.

Table II. Quantum Yields for the Photoaquation Reactions of *cis*-$Ru(NH_3)_4(L)_2^{2+}$ in Aqueous Solution[a]

L	λ_{irr}[b]	$\phi_L/10^{-3}$[c]	$\phi_{NH_3}/10^{-3}$[d]	$\phi_{tot.}/10^{-3}$[e]
4-pic	398	30 ± 1	60 ± 3	90 ± 4
	350	29 ± 1	64 ± 1	93 ± 2
	405	29 ± 3	58 ± 2	87 ± 5
	436	31 ± 1	63 ± 4	94 ± 5
py	313	32 ± 3	53 ± 4	85 ± 7
	365	28 ± 3	53 ± 5	81 ± 8
	405	26 ± 4	57 ± 4	83 ± 8
	436	32 ± 1	66 ± 3	98 ± 4
isn	313	9.0 ± 1	30 ± 1	39 ± 1
	365	8.5 ± 0.1	29 ± 1	38 ± 1
	405	7.8 ± 0.1	26 ± 1	34 ± 1
	436	2.4 ± 0.1	10 ± 1	12 ± 1
	480	1.5 ± 0.1	4.5 ± 0.3	6 ± 0.4
4-acpy	365	5.4 ± 0.6	39 ± 1	44 ± 2
	405	3.8 ± 0.2	30 ± 1	34 ± 1
	436	3.7 ± 0.2	9.7 ± 0.3	13.4 ± 0.5
	480	1.3 ± 0.1	3.6 ± 0.2	4.9 ± 0.3
	519	0.55 ± 0.05	1.2 ± 0.1	1.7 ± 0.1

[a] Reported quantum yields are the average of at least three independent determinations. [b] Irradiation wavelength in nm. Photolyses were carried out in dilute aqueous solutions. $[Ru^{II}] = 10^{-3}$ M, pH ~3.5 adjusted with HCl. [c] Quantum yields, in mol/einstein, determined by selective ion-exchange chromatography of photoreleased free ligands, corrected for dark reaction. [d] Quantum yields, in mol/einstein, determined from increases in solution pH (based on the assumption that one NH_3 is released for each H^+ consumed), corrected for changes induced by release of py, 4-pic, isn, or 4-acpy and for dark reactions. [e] $\phi_{tot.} = \phi_L + \phi_{NH_3}$, in mol/einstein.

The results of Tables II and III show that irradiation of *cis*-$Ru(NH_3)_4(py)_2^{2+}$ and *cis*-$Ru(NH_3)_4(4\text{-pic})_2^{2+}$ at 313, 365, 405, and 436 nm leads to relatively high quantum yields of photosubstitution when they are compared with those of the other complexes. In addition to this, the photosubstitution quantum yields of these two complexes are irradiation wavelength inde-

Table III. Quantum Yields for the Photoaquation Reaction of *cis*-$Ru(NH_3)_4(isn)(L)^{2+}$ in Aqueous Solution[a]

L	λ_{irr}[b]	$\phi_L/10^{-3}$[c]	$\phi_{isn}/10^{-3}$[c]	$\phi_{NH_3}/10^{-3}$[d]	$\phi_{tot.}/10^{-3}$[e]
4-pic	365	12.1 ± 01	3.0 ± 0.1	13.3 ± 0.3	28.4 ± 0.6
	405	8.9 ± 0.2	2.6 ± 0.1	10.0 ± 0.1	21.5 ± 0.4
	436	7.9 ± 0.1	2.4 ± 0.1	8.1 ± 0.2	18.4 ± 0.4
	480	3.9 ± 0.1	1.0 ± 0.1	4.0 ± 0.1	8.9 ± 0.3
py	365	12.5 ± 0.4	3.0 ± 0.2	11.5 ± 0.5	27.0 ± 1
	405	9.7 ± 0.7	2.5 ± 0.1	9.5 ± 0.4	22.0 ± 1
	436	8.4 ± 0.2	2.5 ± 0.1	8.2 ± 0.1	19.1 ± 0.4
	480	3.8 ± 0.1	1.1 ± 0.1	3.8 ± 0.1	8.7 ± 0.3
pz	365	9.9 ± 0.1	8.4 ± 0.3	20.5 ± 0.5	38.8 ± 0.9
	403	4.4 ± 0.2	4.0 ± 0.1	9.3 ± 0.7	18.0 ± 1.0
	436	3.6 ± 0.1	3.1 ± 0.1	7.8 ± 0.2	14.5 ± 0.4
	480	1.7 ± 0.1	1.6 ± 0.1	3.5 ± 0.1	6.8 ± 0.3
4-acpy	365	1.1 ± 0.1	4.8 ± 0.1	9.7 ± 0.1	15.6 ± 0.3
	405	0.9 ± 0.1	2.6 ± 0.1	6.2 ± 0.1	9.7 ± 0.3
	436	0.7 ± 0.1	2.2 ± 0.1	5.0 ± 0.1	7.9 ± 0.3
	480	0.04 ± 0.01	0.7 ± 0.1	1.3 ± 0.1	2.0 ± 0.2
	519	<0.01	<0.4 ± 0.1	0.7 ± 0.1	<1.1 ± 0.2

[a] Reported quantum yields are the average of at least three independent determinations. [b] Irradiation wavelength in nm. Photolyses were carried out in dilute aqueous solutions. $[Ru^{II}] = 10^{-3}$ M, pH ~3.5 adjusted with HCl. [c] Quantum yields in mol/einstein, determined by selective ion-exchange chromatography of photoreleased free ligands, corrected for dark reactions. [d] Quantum yields in mol/einstein, determined from increases in solution pH (based on the assumption that one NH_3 is released for each H^+ consumed), corrected by release of 4-pic, py, isn, pz, or 4-acpy, and for dark reactions. [e] $\phi_{tot.} = \phi_L + \phi_{isn} + \phi_{NH_3}$, in mol/einstein.

Table IV. Molar Ratio of Ligands Released upon Irradiation of *cis*-$Ru^{II}(NH_3)_4(L)(L')$ (L = L')

L	λ_{irr}/nm	L:NH_3
py	313	1:1.7
	365	1:1.9
	405	1:2.2
	436	1:2.1
4-pic	313	1:2
	365	1:2.2
	405	1:2
	436	1:2
isn	313	1:3.3
	365	1:3.4
	405	1:3.3
	436	1:4.2
	480	1:3
4-acpy	365	1:7.2
	405	1:7.9
	436	1:2.6
	480	1:2.8
	519	1:2.2

pendent. This pattern allows the classification of *cis*-$Ru(NH_3)_4(py)_2^{2+}$ and *cis*-$Ru(NH_3)_4(4\text{-pic})_2^{2+}$ as photosubstitution "reactive" complexes. The remaining complexes show relatively lower quantum yields of photosubstitution, which are markedly dependent on the irradiation wavelength. These latter complexes can be classified as "unreactive" toward photosubstitution. For the *cis*-$Ru(NH_3)_4(py)_2^{2+}$ complexes, the total quantum yields are about 90×10^{-3}, while the highest total quantum yield for the "unreactive" complexes is 44×10^{-3} for *cis*-$Ru(NH_3)_4(4\text{-acpy})_2^{2+}$ at 365 nm. In addition to that, the quantum yield dependence on the irradiation wavelength can be seen in a decrease in going from higher energy to lower energy irradiation; as an example, *cis*-$Ru(NH_3)_4(isn)_2^{2+}$ has total quantum yields of 39×10^{-3} at 313 nm and 6×10^{-3} at 480 nm.

Tables IV and V present the ratios of the quantum yields of released ligands. Notably, for each cis complex, a fixed ratio of ligands released, independent of the irradiation wavelength, is observed. A few exceptions are noted in these tables. These are mostly found for complexes giving lower quantum yields where the experimental error is higher.[16] These exceptions occur in

Table V. Molar Ratio of Ligands Released upon Irradiation of *cis*-$Ru^{II}(NH_3)_4(L)(L')^{n+}$ ($L \neq L'$)

L	L'	λ_{irr}/nm	L:L':NH_3
isn	py	365	1:4.2:3.8
		405	1:3.9:3.8
		436	1:3.4:3.3
		480	1:3.5:3.5
isn	4-pic	365	1:4:4.4
		405	1:3.4:3.9
		436	1:3.3:3.4
		480	1:3.9:4.0
isn	pz	365	1:1.2:2.4
		405	1:1.1:2.3
		436	1:1.2:2.5
		480	1:1.1:2.2
isn	4-acpy	365	4.4:1:8.8
		405	2.9:1:6.9
		436	3.1:1:7.1
		480	17.5:1:32.5

cis-$Ru(NH_3)_4(4\text{-acpy})_2^{2+}$, a slight deviation from fixed ratio in *cis*-$Ru(NH_3)_4(isn)(4\text{-pic})^{2+}$, and two points in *cis*-$Ru(NH_3)_4(isn)(4\text{-acpy})^{2+}$.[14]

With regard to the product distribution, the *cis*-$Ru(NH_3)_4L_2^{2+}$, *cis*-$Ru(NH_3)_4(isn)(4\text{-acpy})^{2+}$, and *cis*-$Ru(NH_3)_4(isn)(pz)^{2+}$ ions show ammonia photoaquation as the main photoreaction. However, for the *cis*-$Ru^{II}(NH_3)_4(isn)(L)$ (L = py or 4-pic) complexes, ammonia aquation is lower, and it is similar to L aquation. An additional feature can be seen in the photoproducts distribution in *cis*-$Ru^{II}(NH_3)_4(isn)(L)$ ions. Inspection of Table III indicates that one of the unsaturated ligands is preferentially released. For the *cis*-$Ru(NH_3)_4(isn)(py)^{2+}$ and *cis*-$Ru(NH_3)_4(isn)(4\text{-acpy})^{2+}$ ions, py, 4-pic, and isn are, respectively, the unsaturated ligands released with higher quantum yields; however, for *cis*-$Ru(NH_3)_4(isn)(pz)^{2+}$, pz and isn photoaquations are about the same.

Discussion

The quantum yield values of the photosubstitution reactions of the *cis*-$Ru^{II}(NH_3)_4(L)(L')$ ions show a close parallel with the photosubstitution behavior of similar pentaammine[3] and *trans*-tetraammine[7] complexes. The present data show that the "reactive" complexes are those which have relatively high energy MLCT absorption bands. In contrast, the "unreactive" complexes are those for which at least one unsaturated ligand has a strongly electron-withdrawing substituent and hence shifts the MLCT-1 band to lower energy. These observations are consistent with the excited-state "tuning" model. This model[3] argues that LF excited states (LF*) are responsible for ligand labilization and that the character of the LEES (either LF* or MLCT*) determines the general pattern of the photoaquation quantum yields. Thus, "reactive" complexes have LF* as the LEES and "unreactive" complexes have MLCT* as the LEES. For the "reactive" complexes, *cis*-$Ru(NH_3)_4(py)_2^{2+}$ and *cis*-$Ru(NH_3)_4(4\text{-pic})_2^{2+}$, as it happens in $Ru^{II}(NH_3)_5(py\text{-}X)$, initial excitation into the MLCT bands is followed by relatively efficient intersystem crossing/internal conversion to the LF* lowest state. In low-spin octahedral d^6 systems, LF* involves the population of σ^* (e_g parentage) orbitals along the ligand axes, which account for the substitution behavior. On the other hand, the MLCT excited state (MLCT*) can be described as a short-lived Ru(III) center coordinated to a reduced ligand.[3,17] Since Ru(III) is inert, photosubstitution is not expected to occur from MLCT*, and thus complexes having MLCT* as the LEES are "unreactive". In such complexes, the quantum yield values rise markedly at lower λ_{irr}. The behavior

(16) In ion-exchange determinations, monitored by spectrophotometry, when the concentration of released ligand is too small, the relative error is higher, since there is a small variation in the baseline with elution. In addition to this, in the case of *cis*-$Ru(NH_3)_4(isn)(4\text{-acpy})^{2+}$, the released isn and 4-acpy are eluted together (see Experimental Section), and this implies a higher uncertainty in the relative quantities of each ligand, especially at low concentrations.

(17) Winkler, J. R.; Netzel, T. L.; Creutz, C.; Sutin, N. *J. Am. Chem. Soc.* **1987**, *109*, 2381.

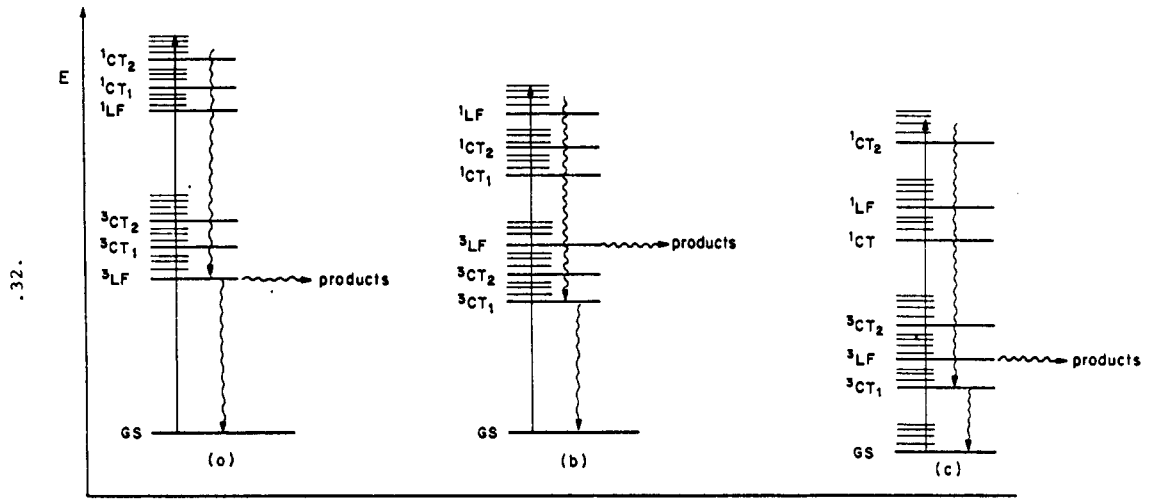

Figure 3. Schematic diagrams of *cis*-$Ru(NH_3)_4LL'$ excited states: (a) "reactive" complex; (b and c) "unreactive" complexes.

is interpreted as reflecting the population and reactivity of some higher energy LF*.

For the $Ru^{II}(NH_3)_5(L)$ complexes there is a crossover from "reactive" to "unreactive" behavior when the λ_{max} of the MLCT absorption band falls above ~460 nm, and a similar pattern was seen for the trans complexes. There is a crossover also in the *cis*-tetraammine complexes. However, for these cis complexes the crossover is determined by the lowest energy MLCT band (MLCT-1). Inspection of Tables I–III indicates that, with the available data, this crossover should be in the region 407–466 nm, since the MLCT-1 band of lowest energy in the "reactive" cis complexes lies at 407 nm, and the MLCT-1 band of highest energy in the "unreactive" cis complexes lies at 466 nm.

The general pattern of irradiation wavelength independent ratio of released ligands points out to a common reactive excited state as the precursor to photosubstitution in each complex. Irradiation at higher energy states is followed by deactivation to one common reactive excited state. Presumably, this is a triplet ligand-field state (^3LF).

Figure 3a depicts a schematic qualitative diagram for a "reactive" complex. In this case, the initial excitation into the MLCT states is followed by relatively efficient intersystem crossing/internal conversion to the lower LF reactive excited state. Figure 3b,c depicts similar diagrams for "unreactive" complexes. For these complexes, initial excitation to higher energy states involves relaxation to the lowest energy MLCT states, and the wavelength dependence of ligand loss can be explained by the internal conversion (from MLCT to LF) along metal–ligand modes competitive in rate with ^3MLCT relaxation.

An exact description of the electronic configurations and states of these complexes is not simple. Symmetry lowering and the effect of back-bonding should be considered in the splitting and energy ordering of the d orbitals. In addition, in the case of *cis*-$Ru^{II}(NH_3)_4(isn)(L)$ complexes, the d_π metal orbitals should be in fact hybrid orbitals of t_{2g} parentage.[10] However, regardless of the number and exact description of the ^3LF states, the results clearly indicate a common reactive state, or an ensemble of equilibrated excited states of the same electronic configuration, as being responsible for the photosubstitution reactions. Thus, the different ligand aquations for the different cis complexes reflect, in fact, different LF excited-state electronic configurations, although one single LF* state, or an ensemble of equilibrated LF of the same electronic configuration, is the reactive state for each complex.

As was pointed out, pentaammines[3] and *trans*-tetraammines[7] have, in general, ammonia aquation as the main photoreaction. In the pentaammines, ammonia aquation comes from labilization of either of the three axes x, y, or z. But in *trans*-$Ru^{II}(NH_3)_4(L)(L')$ complexes the L and L' ligands are in the z axis, so that ammonia aquation must occur through labilization of the x and y axes; this implies that the electronic configuration of the lowest LF excited state in the trans complexes should have a contribution from the $d_{x^2-y^2}$ orbital.[7] On the other hand, py was considered to be a weaker σ donor than NH_3, and then more d_{z^2} population than $d_{x^2-y^2}$ population would be expected in the lowest LF excited state, resulting in greater labilization of L and L'. However, for $Rh^{III}(NH_3)_5(py\text{-}X)$ complexes exclusive py-X photoaquation under LF excitation was observed.[18] The different behavior of Ru(II) was explained[7] in terms of much greater π-back-bonding interaction between the Ru(II) center and the π-unsaturated ligands, which in addition to lowering the energy of d_π orbitals of appropriate symmetry also synergistically increases the σ-donor strength of that ligand, a π-acceptor ligand. Assuming the axes orientation in the cis complexes to be

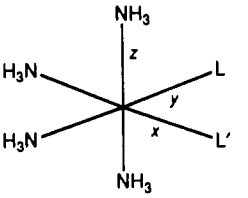

ammonia aquation of the cis complexes can be explained in the same way as it was in the pentaammine and *trans*-tetraammine complexes.

In these cis complexes L and L' photoaquation occur undoubtedly through labilization of the x and y axes (as depicted above), while ammonia aquation can also occur through labilization of the z axis. If the $d_{x^2-y^2}$ orbitals lie lower in energy than the d_{z^2} orbital, ammonia, L, and L' photoaquation could be accounted for by the electronic configuration $(t_{2g})^5(d_{x^2-y^2})^1(d_{z^2})^0$ of the LF excited state. However, if the synergistic effect of back-bonding on σ-bonding is considered enough to place the d_{z^2} orbitals lower in energy and since L and L' aquation requires labilization of x and y axes, the lowest energy LF excited state must then, in this case, have contributions from both d_{z^2} and $d_{x^2-y^2}$ orbitals in the cis complexes *cis*-$Ru^{II}(NH_3)_4(L)(L')$.

Lowest energy LF transitions, according to the above reasoning, involve d_π electrons of t_{2g} parentage going into orbitals of e_g parentage, thus affecting mostly σ-bonding. For a specific complex, the weaker the π-acceptor ability of the axis, the greater the electronic population in this axis. Within an axis, the ligand with weakest π-back-bonding ability would be preferentially released. In all cases of the cis complexes, the z axis is the weakest π-acceptor axis, leading to greater ammonia aquation. In the case of *cis*-$Ru^{II}(NH_3)_4(L)_2$, the x and y axes have the same π-acceptor ability, which is higher than that of the z axis, but in the case of the bis hetero-substituted complexes, *cis*-$Ru^{II}(NH_3)_4(L)(L')$, all

(18) Petersen, J. D.; Watts, R. J.; Ford, P. C. *J. Am. Chem. Soc.* **1976**, *98*, 3188.

three axes have different π-acceptor abilities. Again axes with lower π-acceptor ability will present preferential labilization, and within an axis the weakest π-back-bonding ligand would be preferentially labilized. Assuming that the π-acceptor ability (and the synergistically increased σ-bonding) of the unsaturated ligands follows the order 4-pic < py < isn ≃ pz < 4-acpy, as indicated by the decreasing MLCT transition energy, this is the axes order of π-acceptor ability, and one can see that in a specific complex the ligand aquated with higher quantum yield, or preferentially, is the one that has the lower π-back-bonding ability.

Acknowledgment. This work was supported in part by grants from the CNPq and FAPESP. E.T. acknowledges a research fellowship from the CNPq. L.A.P. acknowledges a doctoral fellowship from the FAPESP and a financial support from the CAPES. We thank Dr. F. A. Leone and the Instituto de Química de Araraquara, UNESP, for the use of their spectrophotometers. We are greatly indebted to Dr. P. C. Ford for helpful discussions, suggestions, and revision of the manuscript.

Registry No. *cis*-$Ru(NH_3)_4(isn)(4\text{-pic})^{2+}$, 132046-85-6; *cis*-$Ru(NH_3)_4(isn)(py)^{2+}$, 60208-54-0; *cis*-$Ru(NH_3)_4(4\text{-acpy})(isn)^{2+}$, 98858-90-3; *cis*-$Ru(NH_3)_4(isn)(pz)^{2+}$, 98858-93-6; *cis*-$Ru(NH_3)_4(4\text{-acpy})_2^{2+}$, 132203-17-9; *cis*-$Ru(NH_3)_4(4\text{-pic})_2^{2+}$, 132046-86-7; *cis*-$Ru(NH_3)_4(py)_2^{2+}$, 46751-30-8; *cis*-$Ru(NH_3)_4(isn)_2^{2+}$, 50573-21-2; *cis*-$Ru(NH_3)_4(pz)_2^{2+}$, 34383-37-4; *trans*-$Ru(NH_3)_4(4\text{-acpy})_2^{2+}$, 115912-47-5; *trans*-$Ru(NH_3)_4(pz)_2^{2+}$, 46751-29-5; *trans*-$Ru(NH_3)_4(pzH)_2^{4+}$, 132046-87-8; *trans*-$Ru(NH_3)_4(isn)(pz)^{2+}$, 60168-50-5; $Ru(NH_3)_5(4\text{-pic})^{2+}$, 19471-55-7; $Ru(NH_3)_5(pz)^{2+}$, 19471-65-9; $Ru(NH_3)_5(pzH)^{3+}$, 19441-21-5; $Ru(NH_3)_5(4\text{-acpy})^{2+}$, 52544-51-1; $Ru(NH_3)_5(isn)^{2+}$, 19471-53-5; $Ru(NH_3)_5(py)^{2+}$, 21360-09-8.

Contribution from the Department of Chemistry, University of Alberta, Edmonton, Alberta, Canada T6G 2G2

Kinetic and Equilibrium Studies of Complexes of Aqueous Iron(III) and Squaric Acid

M. J. Sisley and R. B. Jordan*

Received June 11, 1990

The kinetics and equilibria for the system of aqueous iron(III) and squaric acid (3,4-dihydroxy-3-cyclobutene-1,2-dione) (H_2Sq) have been studied in 1.00 M $HClO_4/LiClO_4$ with concentration ranges of H^+ 0.02–0.10 M, total iron(III) (2.0–7.6) × 10^{-3} M, and total squarate (0.5–2.0) × 10^{-4} M. Spectrophotometric observations lead to the conclusion that two complexes are formed, described by the following reactions with equilibrium constants of 21.4 ± 3.3 and (2.4 ± 0.9) × 10^2 respectively at 23 ± 1 °C: $Fe(OH_2)_6^{3+} + HSq^- \rightleftarrows Fe(OH_2)_5(Sq)^+ + H^+ + H_2O$; $(H_2O)_8Fe_2(OH)_2^{4+} + HSq^- \rightleftarrows (H_2O)_6Fe_2(OH)_2(Sq)^{2+} + H^+ + 2H_2O$. Formation of the iron dimer squarate complex causes the color of solutions to change from bluish purple to bluish red with an absorbance maximum shift from ~540 to lower wavelength as the iron(III) concentration is increased and/or the acidity is decreased. The kinetic observations (25.0 ± 0.1 °C) show a monophasic absorbance change at 545 nm, but a biphasic change at 460 nm, with a 3–5 times larger rate observed at 460 nm. These features are attributed to the formation of the monomeric and dimeric squarate complexes, with rate constants of 5 × 10^4 M^{-1} s^{-1} for $Fe(OH_2)_5OH^{2+} + HSq^-$ or $Fe(OH_2)_6^{3+} + Sq^{2-}$ and 4.5 × 10^4 M^{-1} s^{-1} for $(H_2O)_8Fe_2(OH)_2^{4+} + HSq^-$.

Introduction

Squaric acid (3,4-dihydroxy-3-cyclobutene-1,2-dione, I) is a moderately strong acid ($K_{a1} \approx 0.4$, $K_{a2} = 1.58 \times 10^{-3}$ M)[1] that has some structural analogy to oxalic acid (II) and possibly to ascorbic acid (III). Recent structural studies[2] indicate that

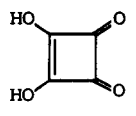

I

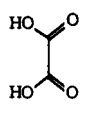

II

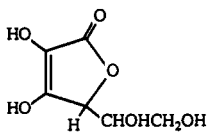

III

squarate forms monodentate complexes and 1,3-bis(metal) complexes rather than 1,2-bidentate chelates with first-row transition metal ions. Solans et al.[2] suggested that squarate does not chelate because of its larger bite distance compared to that of oxalate. A 1,2-bismonodentate structure is found[3] with the bis(μ-hydroxy) dimer of chromium(III), in which squarate acts as a bridge between the two chromium ions. This structure may be especially relevant to the iron(III) chemistry reported here. The analogy to ascorbate with regard to redox properties, has been investigated with pentaammineruthenium(III) complexes.[4]

Tedesco and Walton[1] found that a blue complex is formed in the iron(III)–squaric acid system and that the complex formation can be represented by eq 1, with $K_{f1} \approx 45$ ([iron(III)] ≥ [total squarate] at pH 1.0–1.5). Tedesco and Walton also observed a

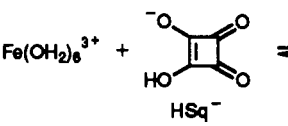

(1)

slow fading of the color, which they attributed to oxidation of squarate, and they noted qualitatively that iron(II) inhibits this reaction.

In many ways, the squarate–iron(III) system is analogous to the ascorbate–iron(III) system. Both form a blue complex whose oxidation is inhibited by iron(II).[5] However, the oxidation with squarate is much slower. Recent work[5] has shown that the initial complexation of ascorbic acid by iron(III) is unusually fast, and this study of the squarate system has been undertaken to seek some explanation for the kinetic observations with ascorbate. It has been found that squarate is unusual in showing clear evidence for complexation with the bis(μ-hydroxy) iron(III) dimer. This product is confirmed by further spectrophotometric studies which reveal that eq 1 does not provide a full representation of the iron(III)–squarate system. In addition, the oxidation stage has been examined in somewhat more detail.

Results

The evolution of our understanding of this system has depended on the interdependence of the stopped-flow and equilibrium

(1) Tedesco, P. H.; Walton, H. F. *Inorg. Chem.* **1969**, *8*, 932.
(2) Solans, X.; Aguiló, M.; Gleizes, A.; Faus, J.; Julve, M. *Inorg. Chem.* **1990**, *29*, 775 and references therein.
(3) Chesick, J. P.; Doany, A. F *Acta Crystallogr.* **1981**, *B37*, 1076.
(4) Bryan, D. M.; Pell, S. D.; Kumar, R.; Clarke, M. J.; Rodriguez, V.; Sherban, M.; Charkoudian, J. *J. Am. Chem. Soc.* **1988**, *110*, 1498.
(5) Xu, J.-H.; Jordan, R. B. *Inorg. Chem.* **1990**, *29*, 4180.

0020-1669/91/1330-2190$02.50/0